Magnesium Technology 2011
Edited by: Wim H. Sillekens, Sean R. Agnew, Neale R. Neelameggham, and Suveen N. Mathaudhu
TMS (The Minerals, Metals & Materials Society), 2011

Experiments and Modeling of Fatigue Damage in Extruded Mg AZ61 Alloy

J.B. Jordon[1], J.B. Gibson[2], M.F. Horstemeyer[2,3]

[1]Department of Mechanical Engineering, The University of Alabama, Tuscaloosa, Al 35487
[2]Center for Advanced Vehicular Systems (CAVS), Mississippi State University, Mississippi State, MS 39762
[3]Department of Mechanical Engineering, Mississippi State University, Mississippi State, MS 39762

Keywords: Fatigue, Structure-Property Relations; Magnesium alloys

Abstract

In this study, structure-property relations with respect to fatigue of an extruded AZ61 magnesium alloy were experimentally quantified. Strain-life experiments were conducted in the extruded and transverse orientations under low and high cycle conditions. The cyclic behavior of this alloy displayed varying degrees of cyclic hardening depending on the strain amplitude and the specimen orientation. The fracture surfaces of the fatigued specimens were analyzed using a scanning electron microscope in order to quantify structure-property relations with respect to number of cycles to failure. Intermetallic particles were found to be the source of fatigue initiation on a majority of fracture surfaces. Finally, a multistage fatigue model based on the relative microstructural sensitive features quantified in this study was employed to capture the anisotropic fatigue damage of the AZ61 magnesium alloy.

Introduction

Given the recent push for energy efficient design, interest in magnesium alloys for automotive structural applications has greatly expanded in recent years. This heightened interest has pushed the materials community to investigate not only cast magnesium but also wrought products for their high strength-to-weight ratio and fatigue resistance. As these wrought products begin to take hold in the automotive community, the need to quantify and make high integrity fatigue predictions of the material performance is of increased importance.

Limited work has been performed recently towards characterizing wrought magnesium cyclic behavior. Cyclic experiments involving extruded AM30, AZ31B, and AZ31 magnesium alloys have been employed to characterize the cyclic response of these materials. These materials were found to have strong cyclic hardening characteristics. In addition, with an increase in total strain amplitude, both plastic strain amplitude and mean stress increased for these alloys. Furthermore, the well known Coffin-Manson law and Basquin's equation were found to correlate with the experimental fatigue results of these alloys quite well [1-6].

The current body of literature on fatigue of wrought magnesium alloys suggests that the mechanisms of fatigue damage evolution are consistent with the well established stages of fatigue for steel and aluminum alloys [7]: incubation, microstructurally small crack growth; physically small crack growth; and long crack growth. Much like wrought aluminum alloys, inclusions can cause fatigue crack incubation in extruded magnesium alloys [8]. Other studies [1-5] on fatigue of wrought magnesium alloys did not explicitly report on the sources of fatigue incubation. However, persistent slip bands and grain boundaries are also thought to be sources of fatigue initiation [1,2,4,9-11]. The mechanisms of twinning on fatigue incubation are unclear, but this is an area of ongoing research. A small level of interest has been shown to the issue of small crack fatigue in wrought magnesium alloys. The inapplicability of the well established linear elastic fracture mechanics (LEFM) parameters (*i.e.,* stress intensity factors) to characterize the growth of fatigue cracks on the order of microns in length is established in wrought magnesium alloys [12,13]. On the other hand, fatigue cracks on the order of millimeters in length and larger are characterized adequately by LEFM parameters [14]. The transition from "small" crack growth to long crack growth has not been established for extruded magnesium alloys. However, the small crack region for cast magnesium alloys appears to be in the range of 60-100 μm [10], which is six to ten times the dendrite cell size.

In regards to the effect of texture on fatigue life in magnesium alloys, the crystallographic orientation appears to have some influence on final failure [9]. Work on other HCP metals was performed on titanium alloys to capture the effects of texture on the fatigue properties [15,16]. Rolling or extruding processes induce strong anisotropy in metals due to preferred crystallographic orientation. This crystallographic orientation has a large effect on twinning and slip in the HCP, therefore affecting the material cyclic behavior. Like the titanium alloys, the effects of texture in wrought magnesium alloys were found to be very important in the cyclic response [8,13,17].

The purpose of this paper is to experimentally quantify the fatigue behavior and the structure-property of an extruded AZ61 magnesium alloy. In addition, a microstructurally-sensitive fatigue model has been developed for wrought alloys based on the experimental results and observations presented here. This model, the MultiStage Fatigue (MSF) model, first proposed by McDowell *et al.* [14], captures the effects of microstructural features as reflected in the incubation and growth stages for both low cycle fatigue (LCF) and high cycle fatigue (HCF). The MSF model was first developed for cast aluminum alloys and was employed to predict the fatigue performance based variation in porosity, grain size, dendrite cell size, and inclusion size and type. The model was later extended to cast magnesium by capturing the network of porosity for AE44 [18], AM50 [19], and AZ91 [20], and was based upon the *in-situ,* scanning electron microscope (SEM) small crack analysis [9-11]. The MSF model was further modified to predict fatigue life in a high strength wrought aluminum alloy by capturing the fatigue crack incubation and growth resulting from iron rich intermetallic particles [18, 21]. These modeling efforts on the wrought aluminum alloy specifically addressed local constrained cyclic microplasticity and crystallographic orientation

[18]. This updated model has also been used for fatigue life predictions of Laser Engineered Net Shaping (LENS) processed steel [22] for A356 and A380-F aluminum alloys [23, 24].

Materials and Experiments

The material used in the study is an extruded AZ61 magnesium alloy. The as-received air-quenched extruded alloy is in the form of an automotive crash rail. The crash rail was extruded at an average temperature of 500 °C and an extrusion exit speed of 4 ft/min. The as-received material was examined with an optical microscope to quantify the initial microstructure in both a transverse material orientation and an extrusion or longitudinal orientation. X-ray diffraction (XRD) was also performed to quantify texture of the as-received material.

Rectangular cross-section tensile specimens were machined in the transverse and longitudinal orientations. The specimens were designed from a scaled ASTM-E8 standard to accommodate the size of the extrudate. The nominal specimens had a 15 mm gage length with a width of 4.35 mm and an as-extruded thickness of 2.5 mm. This design was used for both quasi-static and cyclic tests with the exception that the specimens used for cyclic loads were hand-ground with silicon carbide paper to remove residual stresses and to reduce the machining surface finish effects, which affect the fatigue characteristics.

Monotonic tensile tests were performed using an MTS servo-hydraulic load frame with a capacity of 25 kN. Flat tensile specimens, previously mentioned, were tested in both the longitudinal and transverse orientations in strain control at a rate of 0.01/s in an ambient laboratory environment.

Fully reversed cyclic tests were also performed on a 25 kN Servo-hydraulic MTS load frame in an ambient laboratory environment with relative humidity level of 45%. The fatigue specimens were tested to failure (50% load drop) for both transverse and longitudinal orientations under strain-controlled conditions at 5 Hz and the following strain amplitudes: 0.3%, 0.4%, 0.5%, and 0.6%. The specimens tested at 0.2% and 0.275% strain amplitudes were fatigued at 5 Hz to 10,000 cycles and then the tests were stopped and resumed in load control at 30 Hz to failure.

Fracture surfaces from the fatigued specimens were mounted and Au-Pl sputter-coated to improve imaging quality. The surfaces were then examined in a scanning electron microscope to determine sources of fatigue crack incubation as well as determine regions of small and long crack growth stages. Additionally, chemical analysis was used to determine the composition of areas of interest on the fracture surfaces.

Fatigue Model

The fatigue model employed in this research is the MultiStage Fatigue (MSF) model originally proposed by McDowell et al [14] and later modified by Xue et al [18] and Jordon et al. [23]. The basis of the MSF model is that it comprises fatigue into three distinct regimes: crack incubation, microstructurally small crack (MSC) and physically small crack (PSC) growth, and long crack (LC) growth as shown in Eq. (1).

$$N_{Total} = N_{Inc} + N_{MSC/PSC} + N_{LC}. \quad (1)$$

For brevity's sake, the complete model equations are not shown here, but can be found in [23].

Results and Discussion

The longitudinal orientation was found to have equiaxed grains averaging 37.3 μm, an average particle size of 8.4 μm, an average nearest neighbor distance of 88.5 μm, and a particle area fraction of 0.038 (Figure 1a). The transverse orientation was found to also have equiaxed grains that averaged 48.4 μm, particles that averaged 9.4 μm, a nearest neighbor distance of 104.7 μm, and a particle area fraction of 0.034 (Figure 1b). EDAX chemical analysis of the particles indicates that these particles are Al-Mn based. While not shown here, pole figures of the longitudinal and transverse orientation from XRD results suggest that the AZ61 magnesium alloys are not strongly textured; however, the basal plane is aligned with the longitudinal direction. For further analysis, the comparison of the calculated average Taylor factor for both orientations were made, where the longitudinal direction had an average calculated Taylor value of 2.07 and the transverse direction had an average calculated Taylor value of 2.04. The slight difference in grain size and Taylor factor of both orientations are attributed to the slow extrusion rate that accommodates recrystallization.

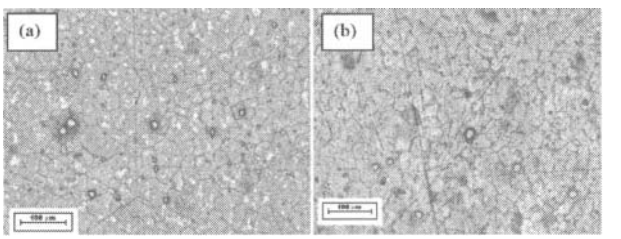

Figure 1. Optical micrographs of as-received extruded AZ61 magnesium alloy polished and etched: (a) longitudinal material orientation with a 37.3μm average grain size (GS), a 8.4μm average particle size (PS), a 0.038 particle area fraction, and a 88.5μm average nearest neighbor distance (NND). (b) Transverse material orientation with a 48.4μm GS, a 9.4μm PS, a 0.034 particle area fraction, and a 104.7μm NND.

Hysteresis and Stress Response

Figure 2 shows the first cycle hysteresis loops for the longitudinal and transverse orientations. The increasing presence of twinning in the first cycles of fatigue loading as the total applied strain amplitude increased was observed for the 0.4% (Figure 2b) and 0.6% (Figure 2c) strain amplitudes. Twinning can accommodate deformation without an increase in stress, which causes the hysteresis loop to have an asymmetric sigmoidal shape to varying degrees in either compression or tension depending on the orientation. A first cycle hysteresis loop for a total applied strain amplitude of 0.2% had a very symmetrical hysteresis loop for both specimen orientations (Figure 2a) while the first cycle hysteresis loop for a total applied strain amplitude of 0.6% had an asymmetric sigmoidal cyclic stress-strain response in tension for the transverse orientation and in compression for the longitudinal specimen orientation due to twin deformation accommodation.

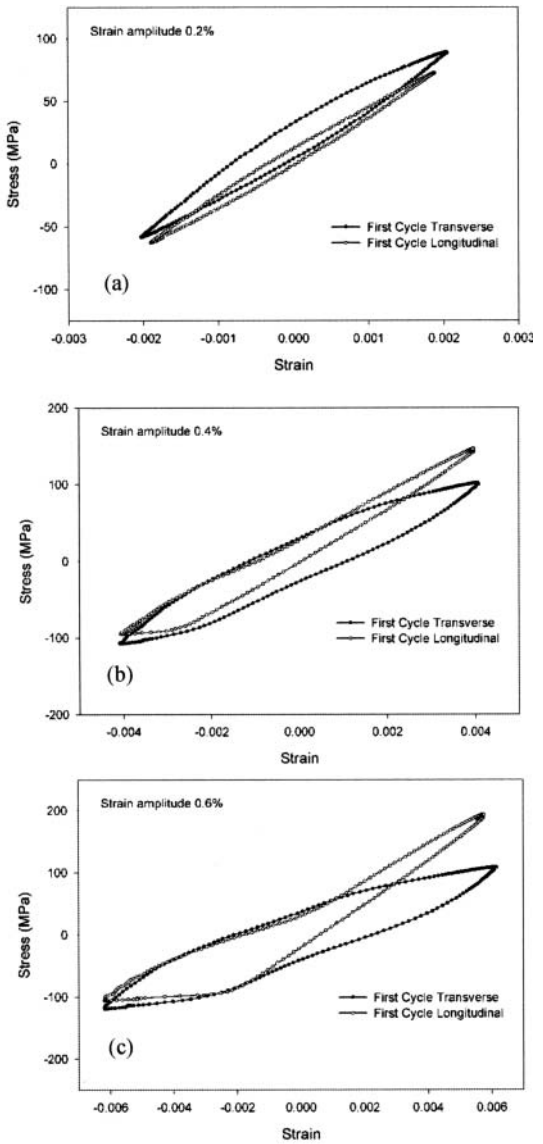

Figure 2. First and half-life cycle hysteresis loops for AZ61 magnesium alloy in the longitudinal and transverse directions with an applied strain amplitude of (a) 0.2%, (b) 0.4%, and (c) 0.6%. Note the stress asymmetry and change in character in the stress-strain response in the 0.4% and 0.6% applied strain amplitudes due to the twinning; these test strain amplitudes were above the cyclic yield stress.

Figure 3. shows the stress amplitude for the longitudinal and transverse orientations versus number of cycles. As the slip becomes the primary deformation mechanism, dislocations begin to pile-up and the material shows a strong hardening response with increased total applied strain amplitude for both orientations as shown in Figure 3a and 3b. This strong observable cyclic hardening is due to the increased plastic strain [1-5]. As the applied strain amplitude decreases, the plastic strain amplitude decreases which in turn diminishes twinning and cyclic hardening alike [25].

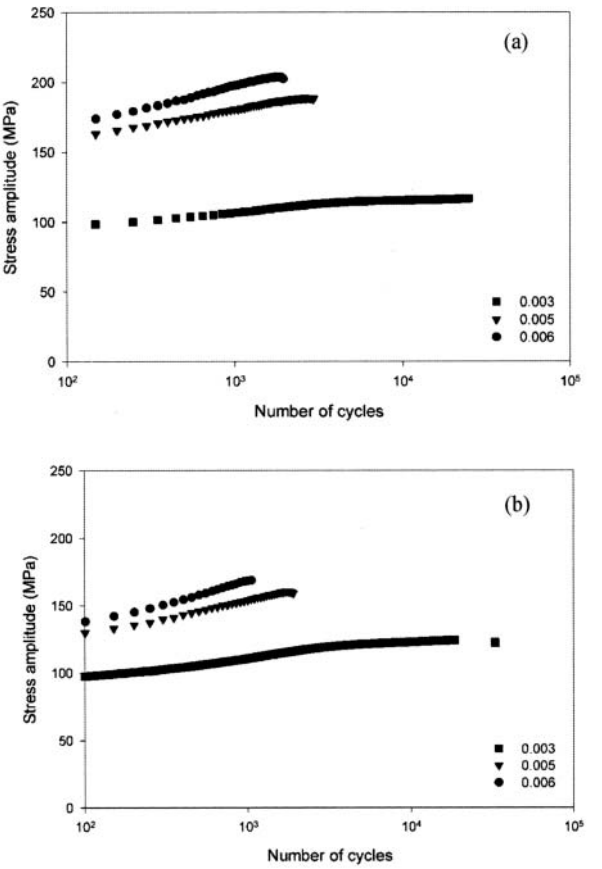

Figure 3. Stress amplitude versus number of cycles for varying applied total strain amplitude of (a) longitudinal and (b) transverse oriented extruded AZ61 magnesium alloy.

Fractography

Extensive fractography was performed on the fatigue fracture surfaces using an SEM to quantify particle sizes that initiated fatigue cracks and the composition of the particles. Fractured particles near the free surface of the specimen were found to be the sites of initiation on most fracture surfaces as shown in Figure 4. Chemical analysis was performed on these particles, and they were found to be Al-Mn based. These particles on the longitudinally oriented specimens had an average equivalent size (derived from the square root of the particle area) of 8.4 μm and a 9.4 μm for the transverse orientation.

SEM fractography conducted in this study resulted in characterization of the distinct stages of fatigue damage: incubation, MSC/PSC, and LC. For low cycle fatigue, the first few hundred cycles of fatigue loading results in particle fracture, which in turn results in incubation of the fatigue crack. The number of cycles for incubation of fatigue cracks is estimated to be approximately 30% based on Bernard et al [26]. SEM analysis of the fracture surfaces showed that a particle near the surface fractured and no debonding was observed. Next, based on comparative textural roughness of the fracture surfaces, the

transition from MSC/PSC to long crack growth was estimated to be approximately 1 mm for both the longitudinal and transverse orientation. Due to the small size of the fatigue specimens, the LC growth was considered to comprise a very small amount of the total life and as such is not included in the modeling portion of this work.

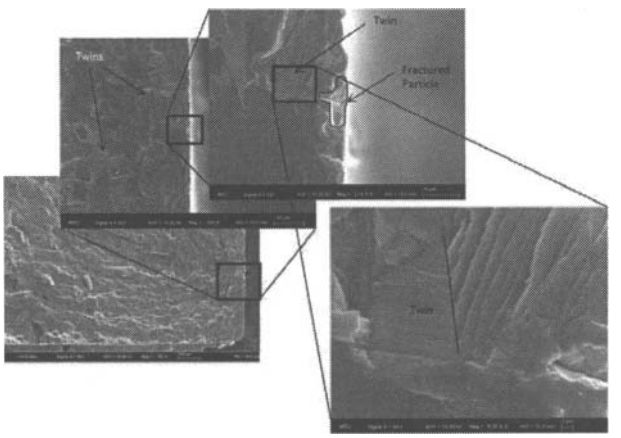

Figure 4. Fracture surface of an extruded AZ61 magnesium alloy longitudinally oriented specimen tested at 0.3% strain amplitude. The scale bar magnitudes from left to right are 1 mm, 200 μm, 100 μm, 20 μm, and 2 μm. Note the twinning on the surface and the particle of initiation (90μm).

Model Correlation

Figure 5 shows the correlations of the MSF model with both the transverse orientation and the longitudinal orientation to experimental data. The difference in the two directions is due to the different grain sizes, particle sizes, yield stresses, and cyclic hardening behavior. All of the other material constants were consistent for both orientation. This is important because it illustrates the sensitivity of the MSF model to capture the effects of microstructural influences on fatigue life. In this particular case, the fatigue life was found to be most sensitive to cyclic hardening parameters related to incubation where the greater the cyclic hardening, the longer the fatigue life.

Figure 6 shows the monotonic stress strain behavior compared to the cyclic stress-strain behavior calculated via companion samples [27]. Maximum tensile stress of the stabilized hysteresis loops was plotted against their respective applied strain amplitudes. Cyclic strain hardening is shown for both the longitudinal and transverse orientations. Cyclic hardening affects the incubation fatigue life by determining the local plastic zone size due to presence of the inclusion. Thus, the differences of the cyclic yield of the two orientations leads to differing local strain fields at the Al-Mn particles responsible for incubating the fatigue cracks.

In an attempt to capture the stochastic nature of the fatigue data, the maximum and minimum particle sizes were employed to obtain error bands for the longitudinal (Figure 7a) and transverse (Figure 7b) directions. In the longitudinal direction, a maximum particle size of 26.4 μm and a minimum of 11 μm were the parameters altered to obtain the bounds of the MSF model for the longitudinal direction. A maximum and minimum particle size of 22 μm and 8.6 μm respectively were used for the transverse orientation bounds. The choices for the selection of the model upper and lower bounds were based on the extreme observable particle sizes taken from the optical analysis and represents the variation of the microstructure. As illustrated in Figure 7, the model captures the upper bounds and lower of the fatigue results, which demonstrates the robustness of the combination of incubation and small crack growth of the MSF model as influenced by varying microstructural features

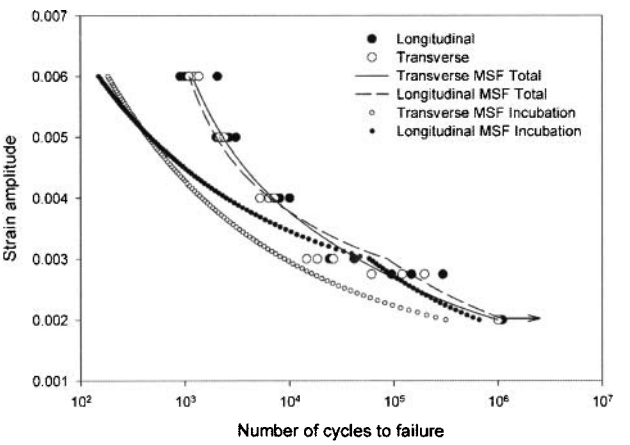

Figure 5. MSF model total life and incubation life comparison with experimental data for extruded AZ61 magnesium alloy.

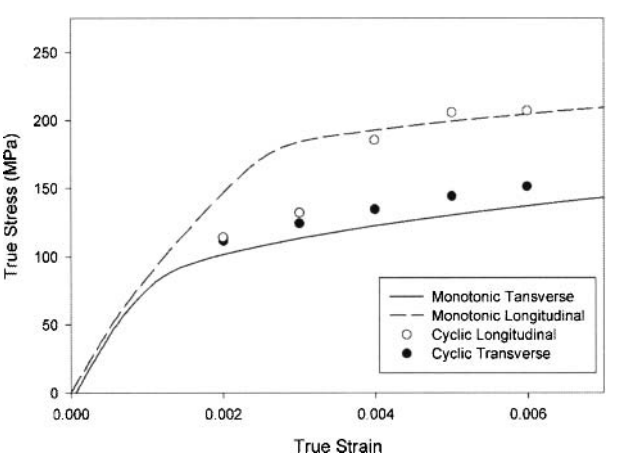

Figure 6 Monotonic tensile stress versus strain behavior and cyclic stress versus strain behavior for fully reversed experiments at half lifetime for an extruded AZ61 magnesium alloy in the transverse and longitudinal material orientations.

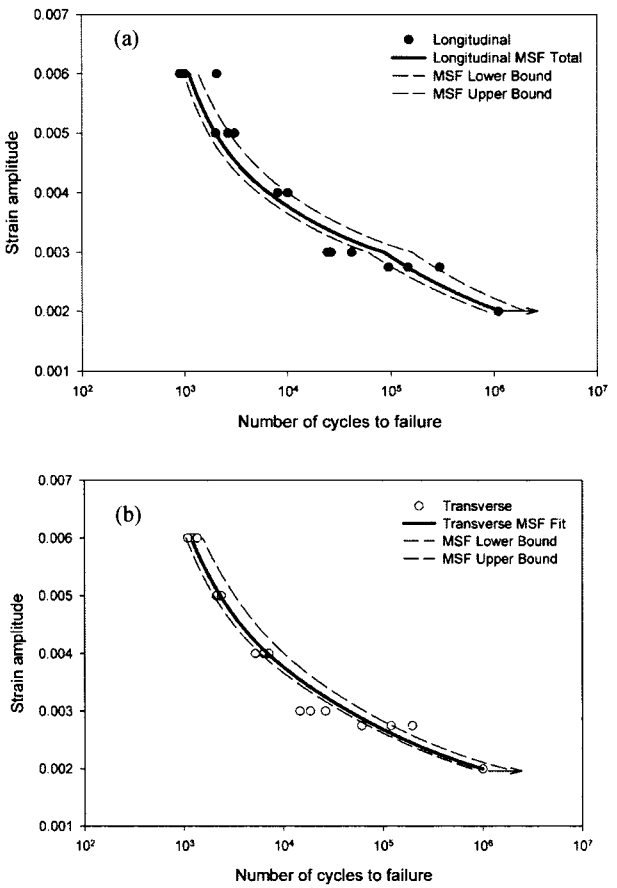

Figure 7 Upper and lower bounds for the MSF model for the (a) longitudinal and (b) transverse directions. These bounds were developed by only varying the particle size by the maximum and minimum of that found on the fracture surfaces.

Conclusions

The monotonic and cyclic behavior of extruded AZ61 magnesium alloy was quantified along with the microstructural characteristics that drove the uncertainty in the mechanical responses. Further, the MultiStage Fatigue (MSF) model was used to capture the strain-life behavior and illustrate the structure-property relationships. The following conclusions were realized from this study.

1) Compressive twinning/detwinning was observed in the longitudinal hysteresis loops due to a tensile stress being induced along the c-axis under compressive loading. Conversely, the transverse hysteresis loops showed tensile twinning/detwinning. Both orientations had a significant Bauschinger effect and were both symmetric and stabilized at the half-life.
2) Fatigue cracks initiated from fractured particles near the free surface.
3) Differences in the longitudinal and transverse orientations were observed on the number of cycles to failure in the high cycle fatigue regime. The longitudinal orientation exhibited greater fatigue resistance compare to the transverse orientation.
4) The MSF model incorporated the differences in grain orientation, grain sizes, particle sizes, and cyclic hardening parameters in order to capture the differences in the longitudinal and transverse fatigue behavior of an extruded AZ61 magnesium alloy. We note that the other material constants were not changed for the incubation and MSC regimes. Also, the MSF model captured the upper and lower bounds on the strain-life curve by simply employing the maximum and minimum particle sizes found in the as-received material. Thus, illustrating the effects of the microstructural content on the fatigue properties.

Acknowledgments - The authors would like to recognize Richard Osborne, James Quinn, Xuming Su, John Allison, Robert McCune, Don Penrod, and Matthew Castanier for their encouragement of this study. This material is based upon work supported by the Department of Energy and the National Energy Technology Laboratory under Award Number No. DE-FC26-02OR22910, and the U.S. Army TACOM Life Cycle Command under Contract No. W56HZV-08-C-0236 through a subcontract with Mississippi State University, and was performed for the Simulation Based Reliability and Safety (SimBRS) research program. This report was prepared as an account of work sponsored by an agency of the United States Government. Neither the United States Government nor any agency thereof, nor any of their employees, makes any warranty, express or implied, or assumes any legal liability or responsibility for the accuracy, completeness, or usefulness of any information, apparatus, product, or process disclosed, or represents that its use would not infringe privately owned rights. Reference herein to any specific commercial product, process, or service by trade name, trademark, manufacturer, or otherwise does not necessarily constitute or imply its endorsement, recommendation, or favoring by the United States Government or any agency thereof. The views and opinions of authors expressed herein do not necessarily state or reflect those of the United States Government or any agency thereof. Such support does not constitute an endorsement by the Department of Energy of the work or the views expressed herein. UNCLASSIFIED: Dist A. Approved for public release.

References

1. Begum S, Chen DL, Xu S, Luo Alan A. Strain-controlled low-cycle fatigue properties of a newly developed extruded magnesium alloy. Metall Mater Trans A 2008;39A:3014-26.

2. Begum S, Chen DL, Xu S, Luo Alan A. Low cycle fatigue properties of an extruded AZ31 magnesium alloy. Int J Fatigue 2009;31:726-35.

3. Begum S, Chen DL, Xu S, Luo Alan A. Low cycle fatigue properties of an extruded AZ31 magnesium alloy. Int J Fatigue 2009;31:726-35.

4. Lin XZ, Chen DL. Strain controlled cyclic deformation behavior of an extruded magnesium alloy. Mater Sci Eng A 2008;496:106-13.

5. Lin XZ, Chen DL. Strain hardening and strain-rate sensitivity of an extruded magnesium alloy. J Mater Eng Perform 2008;17:894-901.

6. Hasegawa S, Tsuchida Y, Yano H, Matsui M. Evaluation of low cycle fatigue life in AZ31 magnesium alloy. Int J Fatigue 2007;29:1839-45.

7. Suresh S. Fatigue of materials. United Kingdom: Cambridge University Press; 1998

8. Bernard JD, Jordon JB, Horstemeyer MF, El Kadiri H, Baird J, Lamb D, Luo AA. Structure-property relations of cyclic damage in a wrought magnesium alloy. Scr Mater. In Press, 2010.

9. Gall K, Biallas G, Maier HJ, Gullett P, Horstemeyer MF, McDowell DL. In-Situ observations of low-cycle fatigue damage in cast AM60B magnesium in an environmental scanning electron microscope. *Metall Mater Trans A* 2004a;35:321-31.

10. Gall K, Biallas G, Maier HJ, Gullett P, Horstemeyer MF, McDowell DL, Fan J. In-Situ observations of high cycle fatigue mechanisms in cast AM60B magnesium in vacuum and water vapor environments. Int J Fatigue 2004b;26:59-70.

11. Gall K, Biallas G, Maier HJ, Horstemeyer MF, McDowell DL. Environmentally influenced microstructurally small fatigue crack growth in cast magnesium. Mater Sci Eng A 2005;396:143-54.

12. Tokaji K, Kamakura M, Ishiizumi Y, Hasegawa N. Fatigue behavior and fracture mechanisim of a rolled AZ31 magnesium alloy. Int J Fatigue 2004;26:1217-24.

13. Sajuri ZB, Miyashita Y, Hosokai Y, Mutoh Y. Effects of Mn content and texture on fatigue properties of as-cast and extruded AZ61 magnesium alloys. Int J Mech Sci 2006;48:198-209.

14. McDowell DL, Gall K, Horstemeyer MF, Fan J. Microstructure-based fatigue modeling of cast A356-T6 alloy. Eng Fract Mech 2003;70:49-80.

15. Bache MR, Evans WJ, Randle V, Wilson RJ. Characterization of mechanical anisotropy in titanium alloys. Mater Sci Eng A 1998;A257:139-44.

16. Whittaker MT, Evans WJ, Lancaster R, Harrison W, Webster PS. The effect of microstructure and texture on mechanical properties of Ti6-4. Int J Fatigue 2009;31:2022-30.

17. Chamos AN, Pantelakis SG, Haidemenopoulos GN, Kamoutsi E. Tensile and fatigue behavior of wrought magnesium alloys AZ31 and AZ61. Fatigue Fract Eng Mater Struct 2008;31:812-21.

18. Xue Y, McDowell DL, Horstemeyer MF, Dale MH, Jordon JB. Microstructure-based multistage fatigue modeling of aluminum alloy 7075-T651. Eng Fract Mech 2007;74:2810-23.

19. El Kadiri H, Xue Y, Horstemeyer MF, Jordon JB, Wang PT. Identification and modeling of fatigue crack growth mechanisms in a die-cast AM50 magnesium alloy. *Acta Mater* 2006;54:5061-76.

20. Horstemeyer MF, Yang N, Gall KA, McDowell DL, Fan J, Gullett P. High cycle fatigue on a die cast AZ91E-T4 magnesium alloy Acta Mater 2004;52:1327-36.

21. Xue Y, Horstemeyer MF, McDowell DL, El Kadiri H, Fan J. Microstructure-based multistage fatigue modeling of a cast AE44 magnesium alloy. Int J Fatigue 2007;29:666-76

22. Xue Y, Pascu A, Horstemeyer MF, Wang L, Wang PT. Microporosity effects on cyclic plasticity and fatigue of LENS-processed steel. Acta Mater 2010;58:4029-38.

23. Jordon JB, Horstemeyer MF, Yang N, Major JF, Gall KA, Fan J. Microstructural inclusion influence on fatigue of a cast A356 aluminum alloy. Metall Mater Trans A 2010;41A:356-363

24. Xue Y, Burton CL, Horstemeyer MF, McDowell DL, Berry JT. Multistage fatigue modeling of cast A356-T6 and A380-F aluminum alloys. Metall Mater Trans B 2007;38B:601-6.

25. El Kadiri H, Oppedal AL. A crystal plasticity theory for latent hardening by glide twinning through dislocation transmutation and twin accommodation effects. J Mech Phys Solids 2010;58:613–24

26. Bernard JD, Jordon JB, Horstemeyer MF. Small fatigue crack growth observations in a wrought magnesium alloy, TMS 2011 Annual Meeting and Exhibition, [submitted].

27. Bannantine JA, Comer JJ, Handrock JL. Fundamentals of metal fatigue analysis. USA: Prentice Hall; 1990.